

Average scattering entropy for periodic, aperiodic and random distribution of vertices in simple quantum graphs

Alison A. Silva^a, Fabiano M. Andrade^{a,b,*} and D. Bazeia^c

^aUniversidade Estadual de Ponta Grossa, Programa de Pós-Graduação, Ponta Grossa 84030-900, Paraná, Brazil

^bUniversidade Estadual de Ponta Grossa, Departamento de Matemática e Estatística, Ponta Grossa 84030-900, Paraná, Brazil

^cUniversidade Federal da Paraíba, Departamento de Física, João Pessoa 58051-900, Paraíba, Brazil

ARTICLE INFO

Keywords:

Entropy
Scattering
Quantum graphs
Topology

ABSTRACT

This work deals with the average scattering entropy of quantum graphs. We explore this concept in several distinct scenarios that involve periodic, aperiodic and random distribution of vertices of distinct degrees. In particular, we compare distinct situations to see how they behave as we change the arrangements of vertices and the topology of the proposed structures. The results show that the average scattering entropy may depend on the number of vertices, and on the topological disposition of vertices and edges of the quantum graph. In this sense, it can be seen as another tool to be used to explore topological effects of current interest for quantum systems.

1. Introduction

The main aim of the present work is to study specific properties of quantum graphs [1]. In particular, we will investigate the average scattering entropy (ASE), a concept based on the Shannon entropy [2] which was recently introduced in Ref. [3], that allows us to associate a global quantity to a given quantum graph (QG). The ASE is calculated from the scattering properties of a QG, so we take advantage of the scattering Green's function approach for QG developed in Refs. [4, 5] to implement the investigation. Here we focus on the calculation of this quantity in several distinct situations, to show that the procedure works adequately and also, to see how it changes as we modify the array of vertices and leads following some general possibilities, as the periodic, aperiodic and random distribution of vertices in the graphs. The interest is to add more information concerning the behavior of the ASE as we change the way the vertices dispose themselves in each QG. Besides, we want to add more motivation with the study of QG that may be directly connected to the study of quantum walks [6–10], quantum walks in optical lattices [11], and networks of soft active matter [12–14].

As one knows, a QG is a structure associated with an arbitrary arrangement of vertices, edges and leads, and in Fig. 1 we depict two quantum graphs, both having 11 vertices and 19 edges, but in the structure on the right one attaches 8 leads, as appropriate for the study of scattering properties of quantum graphs. Beyond paying closer attention to the periodic, aperiodic and random distribution of vertices in the QG, we will also deal with topology and geometry, to see how they can contribute to change the ASE contents of each QG. Although the periodic array of vertices in a QG is of direct interest to physics, the possibility of considering

aperiodic and random distribution of vertices is also of interest, although more involved. This is related to the possibility to select two very simple but distinct structures and use them to build distinct arrangements of vertices and edges. We name these elementary structures as α and β , and depict their forms in Fig. 2. These QGs were already studied in [3] and despite their simplicity, they engender interesting scattering properties and the respective ASE values are calculated at the end of Sec. 2

In the investigation developed in Ref. [3], we have introduced the ASE owing to associate a global value connected to the complicated energy-dependent scattering probabilities of a given quantum graph, based on the Shannon entropy. As one knows, for a system having a set of n equally probable states, the Shannon entropy gives $\log_2 n$, so it increases as the number of states increases. As a consequence, a fair die has more information value than a fair coin. In the case of the ASE, we are dealing with the scattering probabilities of open quantum graphs (see Sec. 2 for details), but its interpretation is similar to the interpretation of the Shannon entropy.

In this work, we use the α and β structures to build periodic, aperiodic and random arrangements on the line and on the circle and study how the ASE changes as we add more and more vertices to the QGs. A motivation of current interest is that α and β can be seen as a quantity having

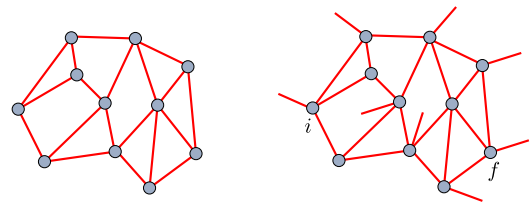


Figure 1: (Color online) Closed quantum graph with 11 vertices and 19 edges (left) and the associated open quantum graph with 8 leads added (right), with i and f identifying the entrance and exit scattering channels.

*Corresponding author

✉ fmandrade@uepg.br (F.M. Andrade)

ORCID(s): 0000-0003-3552-8780 (A.A. Silva); 0000-0001-5383-6168 (F.M. Andrade); 0000-0003-1335-3705 (D. Bazeia)



Figure 2: (Color online) Two very simple quantum graphs with two external leads. They are the α (left) and β (right) structures, and have a single vertex of degree 3 (left) or 4 (right) attached to one or two dead end vertices of degree 1, respectively.

two distinct conformations as in a two-state quantum system. This possibility opens an interesting route of investigation, which is directly related to the study of quantum walks using neutral atoms trapped in optical lattices, for which the investigations [11, 15] may be considered for applications of practical interest. To make the investigation more general, we also study other arrangements, in particular the two-dimensional case where the network conforms itself as flat and curved defect-like structure, which is directly related to the model investigated in Ref. [14], that is of interest to the study of pattern formation in systems of active soft matter [12].

We also study other networks which require working in two and three dimensions. Examples are the sequences of squares which can be disposed as flat stripe-like configurations in two dimensions (2D), and the regular triangular prisms that form triangular tube-like configurations in three dimensions (3D). These arrangements will also be investigated in this work, to see how they contribute to change the corresponding ASE values, as we increase the number of elements in 2D and 3D networks.

In addition to the direct interest related to thermodynamics, statistical and quantum information, there are several other possibilities connected to the subject of the present work. In high energy physics, for instance, the concept of configurational entropy introduced in Ref. [16], which is also based on the Shannon entropy, has been used in several distinct directions to analyse stability of physical systems that are localized in space: in the investigation of mesons propagating in chiral and gluon condensates in a gravity background [17], in the examination of heavy mesons in the quark gluon plasma [18, 19], in the study of the magnetic structure of skyrmions in planar magnetic materials [20, 21], in the investigation of the soft wall background as a function of the temperature [22], the mass spectra of meson resonances [23] and anti-de Sitter graviton stars [24], to quote just a few recent works on the subject.

We organize the present investigation as follows: in the Sec. 2 we review the scattering in QGs using the Green's function approach, and the concept concerning the ASE on general grounds. After briefly describing the formalism, we then include in Sec. 3 the main results of the work, calculating the ASE for several open and closed arrangements of vertices in distinct scenarios, involving periodic, aperiodic and random distributions of elementary structures, and other two and three dimensional arrangements of vertices, edges

and external leads. We then end the work in Sec. 4, where we add some comments and suggest new lines of research of current interest related to the subject of study in the present investigation.

2. Scattering in quantum graphs

As one knows, a QG can be described as a triple $\{\Gamma(V, E), H, BC\}$, consisting of a metric graph $\Gamma(V, E)$, a differential operator H and a set of boundary conditions, BC [1]. A metric graph $\Gamma(V, E)$ is a set of v vertices, $V = \{1, \dots, v\}$, and a set of e edges, $E = \{e_1, \dots, e_e\}$, where each edge links a pair of vertices $e_s = \{i, j\}$, with non-negative lengths $\ell_{e_s} \in (0, \infty)$. Here we consider the free Schrödinger operator $H = -(\hbar^2/2m)d^2/dx^2$ acting on each edge and the most natural set of boundary conditions on the vertices, namely, the Neumann boundary conditions. The graph topology is defined by its adjacency matrix $A(\Gamma)$ of dimension $v \times v$; their elements $A_{ij}(\Gamma)$ are 1 if the vertices i and j are connected and 0 otherwise. We introduce an open QG, Γ^l , which is suitable to study scattering problems, by adding l leads (semi-infinite edges) to its vertices, as illustrated in Fig. 1 (right). The open QG Γ^l can then be used to describe a scattering system with l scattering channels which is characterized by the energy-dependent global scattering matrix $\sigma_{\Gamma^l}(k)$, where k is the wave number, which is related to the energy by the standard expression $E = \hbar^2 k^2 / 2m$, and the matrix elements are given by the scattering amplitudes $\sigma_{\Gamma^l}^{(f,i)}(k)$, where i and f represents the entrance and exit scattering channels, respectively.

2.1. Scattering Amplitudes

The calculation of the scattering amplitudes $\sigma_{\Gamma^l}^{(f,i)}(k)$ is based on the scattering Green's function approach developed in Refs. [4, 5]. This procedure was recently used to study narrow peaks of full transmission and transport in simple quantum graphs in Refs. [25, 26], which has inspired us to introduce the ASE in Ref. [3] and explore it in the present study. In this manner, the scattering amplitudes are given by

$$\sigma_{\Gamma^l}^{(f,i)}(k) = \delta_{fi} r_i + \sum_{j \in E_i} A_{ij} P_{ij}^{(f)}(k) t_i, \quad (1)$$

where i and f are the entrance and exit scattering channels, E_i is the set of neighbor vertices connected to i , and r_i and t_i are the reflection and transmission amplitudes at the vertex i , which for Neumann boundary conditions (Neumann vertices), are given by [27]

$$r_i = \frac{2}{d_i} - 1, \quad t_i = \frac{2}{d_i}, \quad (2)$$

where $d_i \geq 2$ is the degree of the vertex i (the total number of edges and/or leads attached to it). Neumann vertices of degree one have $r_i = 1$. The quantities $P_{ij}^{(f)}(k)$ are the families of paths between the vertices i and j , and they are

given by

$$P_{ij}^{(f)}(k) = z_{ij}\delta_{fj}t_j + z_{ij}P_{ji}^{(f)}(k)r_j + z_{ij}\sum_{l \in E_j^{i,f}} A_{jl}P_{jl}^{(f)}(k)t_j, \quad (3)$$

where $z_{ij} = e^{ik\ell_s}$ with ℓ_s representing the length of the edge $e_s = \{i, j\}$ connecting i and j ; also, $E_j^{i,f}$ stands for the set of neighbors vertices of j but with the vertices i and f excluded. The family $P_{ji}^{(f)}(k)$ is obtained from the above equation by swapping $i \leftrightarrow j$ and the number of family of paths is always twice the number of edges of the graph under investigation. The family of paths altogether form an inhomogeneous system of equations and its solution leads to the scattering amplitude $\sigma_{\Gamma^l}^{(f,i)}(k)$ [4].

2.2. Average Scattering Entropy

Consider the scattering on a QG Γ^l as described above. By fixing the entrance channel, say i , this scattering system is characterized by l quantum amplitudes, which are given by Eq. (1). This defines a set of l scattering probabilities

$$p_{\sigma_{\Gamma^l}}^{(j)}(k) = |\sigma_{\Gamma^l}^{(j,i)}(k)|^2, \quad (4)$$

for a quantum particle entering the graph with wave number k through the fixed vertex i , and exiting the graph by some other vertex j (also including the vertex i itself). These probabilities fulfills the constrain

$$\sum_{j=1}^l p_{\sigma_{\Gamma^l}}^{(j)}(k) = 1, \quad (5)$$

which is a consequence of the probability conservation in the scattering process, or better, of the unitarity of the scattering matrix. Thus, the scattering process that occurs in a QG is analogous to a random variable with l possible outcomes. With this in mind, for graphs where their scattering probabilities are periodic, in Ref. [3] we introduced the ASE which is given by

$$\bar{H}(\sigma_{\Gamma^l}) = \frac{1}{K} \int_0^K H_{\sigma_{\Gamma^l}}(k) dk, \quad (6)$$

where K is the period of the scattering probability, and

$$H_{\sigma_{\Gamma^l}}(k) = - \sum_{j=1}^l p_{\sigma_{\Gamma^l}}^{(j)}(k) \log_2 p_{\sigma_{\Gamma^l}}^{(j)}(k), \quad (7)$$

is the Shannon entropy which encodes the informational content of the scattering process on a QG as a function of k . Therefore, the ASE encodes all the complicated behavior of the scattering probabilities of a QG into a single number. It is interesting to observe that when the scattering probability for all the l scattering channels is equal to $p_{\sigma_{\Gamma^l}}^{(j)}(k) = 1/l$, $H_{\sigma_{\Gamma^l}}(k)$ assumes its maximum value $\log_2 l$. On the other hand, the minimum occurs when all the scattering probabilities are 0 but one is 1, which corresponds to a full reflection or a full transmission.

Evidently, the probability displayed in Eq. (4) also depends on the incoming channel, and so does the ASE in Eq. (6) and the entropy in Eq. (7). Moreover, we notice here that associating the entries of a unitary matrix with transition probabilities has also been done in Ref. [28] in the context of stochastic dynamics on a graph, proposing to study unitary matrix ensembles defined in terms of unitary stochastic transition matrices associated with Markov processes on graphs, which may motivate another line of study. We also notice that the above procedure can be directly used to calculate the ASE values for the two simple graphs displayed in Fig. 2: the α and β structures give 0.503258 and 0.557305, respectively. We can verify that these results are independent of the boundary conditions for the dead end vertices of degree 1 being Dirichlet or Neumann; see, e.g., Ref. [3] for other details on this issue.

3. Results

Let us now investigate some specific QG configurations to see how the ASE behaves as we change the number of vertices and the corresponding degrees, and the way they are assembled on the line and on the circle, with periodic, aperiodic and random dispositions, and in other situations having geometric and spatial modifications. The several possibilities investigated are described in the subsections that follows.

3.1. Periodic arrangements

We start using a regular distributions of vertices of degree $d = 3$ and $d = 4$ on the line, generically represented by α_n and β_n , with α and β already introduced in Fig. 2, and with $n = 1, 2, 3, \dots$ standing for the number of replications in the arrangements. We are considering ideal vertices, and we use Neumann boundary conditions for the dead end vertices of degree 1, wherever they appear in the quantum graphs. Also, in these arrangements, all the edges connecting two vertices have the same length, i.e., we are considering *equilateral* QGs. An illustration is depicted in Fig. 3 for the cases α_4 and β_3 . We take advantage of the results obtained in Ref. [3] and display in red and blue in Fig. 4 the several values of the ASE with α (blue) and β (red) vertices on the line. We notice that the value rapidly diminishes and saturates to a constant as n , the number of replications, increases to larger and larger values. Also, it is always higher for the arrangements with β vertices. In this sense, one sees that although the degree d is significant, the number of replications or the size of the lattice seems to play no important role for n greater than 3. This means that the ASE is importantly affected by the degree of the vertices, although it is practically insensitive to the addition of extra vertices in chains of three or more vertices. However, it varies significantly when one changes from one to two replications, meaning that small structures feel the ASE more importantly.

Another situation of interest concerns periodic arrangement of vertices on the circle, and here we study the case with α and β vertices, and compare the results with the results already obtained on the line. In Fig. 5 we display two

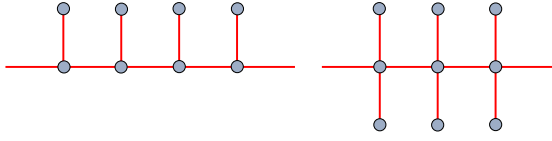


Figure 3: (Color online) The α_4 (left) and β_3 (right) arrangements which we use to illustrate the general case on the line.

QGs to illustrate the general situation in the two cases on the circle. We notice that all the degree 1 vertices are attached to vertices of degree three for the α configurations, and four, for the β configurations. On the circle we then have ring-like structures formed by vertices of degree 3 and 4, for the α , and β structures, respectively, and we then have several different ways to probe them under scattering adding two external leads. Here we will consider the following two cases, which we believe are of interest for the transport in molecules in break junctions [29, 30] and in microwave networks [31], for instance. The first case refers to the addition of two external leads, one at one of the vertices in the ring-like structure, and the other one at the neighbor vertex in the ring. This is illustrated in Fig. 5, left, with the two external leads, and we identify this type of arrangement as Circle. In the second case, we also attach two external leads, one to a vertex of degree 1 which is connected to a vertex in the ring, and the other to a vertex of degree 1 which is connected to the neighbor vertex in the ring. This is also illustrated in Fig. 5, right, with the two external leads, and we identify these configurations as Circle2. We notice that in the first case, we keep the total number of vertices and edges, but we increase by 1 the degree of two vertices in the ring; and in the second case, we remove 2 vertices of degree 1 and two edges, since vertices of degree 2 are transparent, but we keep the degree of the vertices in the ring.

Now, we follow the approach in Ref. [3] and depict the results in Figs. 6 and 7 on the line and on the circle in the first case. We notice that the values on the circle are always higher than on the line. We also notice from Figs. 6 and 7 that for $n \leq 7$, the ASE varies more significantly on the circle than

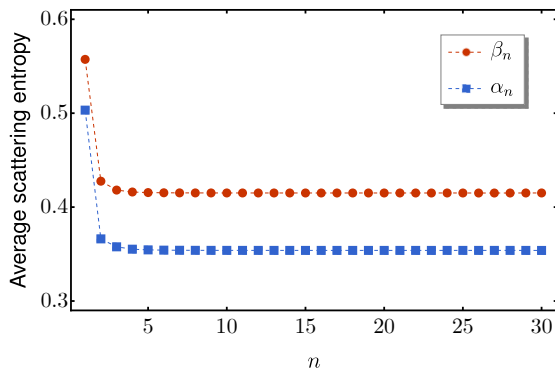


Figure 4: (Color online) Average scattering entropy of the quantum graphs α_n (blue) and β_n (red) on the line, for several values of n .

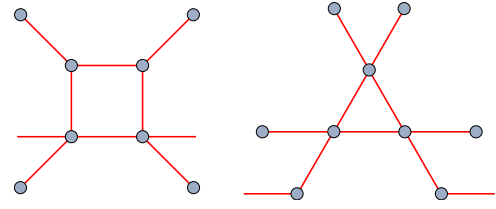


Figure 5: (Color online) Two quantum graphs with α_4 (left) and β_3 (right), which illustrate the general case of periodic structures on the circle.

on the line. We also consider the ASE for configurations of the Circle2 type. The results appear in Fig. 8, and we notice that the results for β configurations are always higher than in the case of the α type.

3.2. Aperiodic arrangements

Let us now consider QG configurations with aperiodic compositions of α and β vertices, on the line and on the circle. In order to implement the aperiodic disposition, we follow [32] and choose α and β with the following rules: $\alpha \rightarrow \alpha\beta$ and $\beta \rightarrow \alpha$; one starts with α and implement the rules, to get the sequences: α , $\alpha\beta$, $\alpha\beta\alpha$, $\alpha\beta\alpha\alpha\beta$, etc. This reproduces the Fibonacci sequence of numbers, so using the α and β vertices, one can then construct aperiodic sequences of vertices on the line and on the circle. In Ref. [32] one can find interesting physical motivation and experimental implementation for these aperiodic arrangements of vertices. The fact that α and β correspond to vertices of two different degrees, it allows us to associate them to two different states of each individual vertex. This can be used to make a direct connection between arrangements of vertices and optical lattices of Rubidium neutral atoms, for instance, since Rubidium may be treated as a two-state system; see, e.g., Ref. [11].

Motivated by the possibility of using aperiodic arrangements of vertices, we then implement the calculation of the ASE. The results are depicted in Fig. 9 on the line and on the

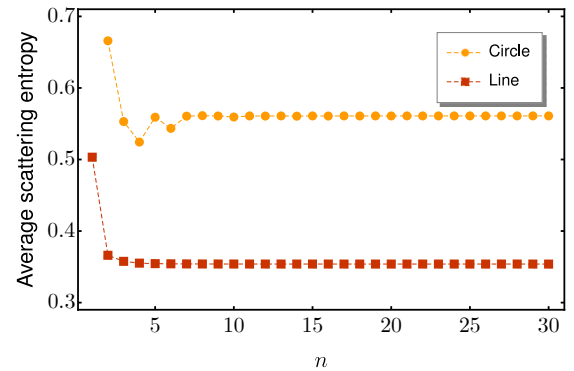


Figure 6: (Color online) Average scattering entropy of quantum graphs formed by α vertices of degree 3 on the line (red) and on the circle (orange).

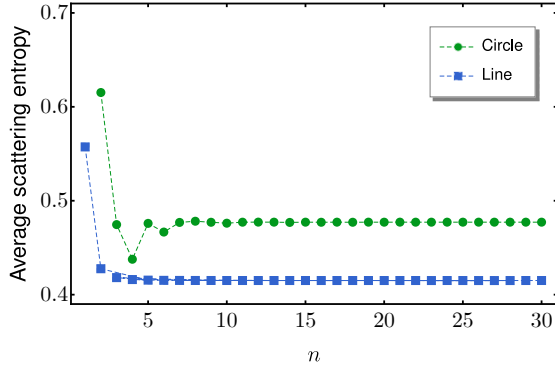


Figure 7: (Color online) Average scattering entropy of quantum graphs formed by β vertices of degree 4 on the line (blue) and on the circle (green).

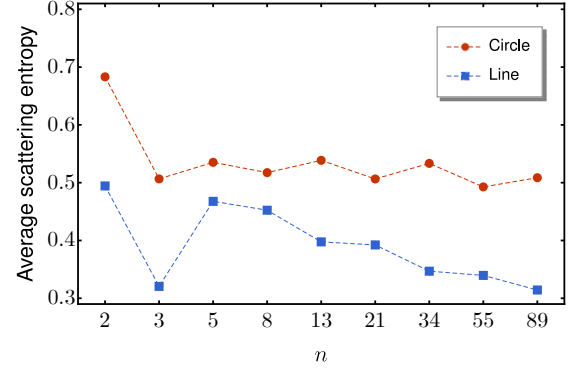


Figure 9: (Color online) Average scattering entropy of quantum graphs on the line (blue) and on the circle (red) identified by a Fibonacci number, as explained in the text.

circle, for several Fibonacci numbers. Notice that the horizontal axis in Fig. 9 is out of scale, to leave room to display several Fibonacci numbers. Moreover, we remind that the Fibonacci sequence is given by 1, 1, 2, 3, 5, 8, 13, 21, ..., with the property that the sum of any two neighbor elements gives the next one, that is, $x_i + x_{i+1} = x_{i+2}$, with $i = 1, 2, 3, \dots$. We also display the results for configurations of the Circle2 type in Fig. 10. We compare the results for the red dots in Figs. 9 and in Fig. 10 to see that they engender similar qualitative behavior, although in the Circle2 case the variations are more significant.

3.3. Random arrangements

We now focus on the case where random distributions of α and β vertices are considered. We also consider the two cases on the line and on the circle, but now, due to the random nature of the distribution of α and β vertices, we considered the cases with 13, 21, 34, 55 and 89 vertices. Evidently, we can choose other values, but the selected Fibonacci numbers are taken to ease comparison with the results of the previous, aperiodic arrangements. To calculate the results displayed in Fig. 11, we considered from each

ensemble a sample of 100 different random choices for the random sequence of α and β vertices. The dots depicted in Fig. 11 represent the mean or expected values, and the corresponding (almost invisible) bars stand for the standard deviations. The results show that the ASE on the Circle are higher than on the line. We also depict in Fig. 12 the case with random arrangements of α and β vertices for configurations of the Circle2 type.

3.4. Other 2D and 3D results

We can also investigate other planar 2D and spatial 3D arrangements of QGs. We first consider the cases having the planar γ and the spatial δ structures, the first with 4 vertices and 5 edges, and the second with 5 vertices and 9 edges; see Fig. 13 for an illustration. We notice that in the 2D case, all the vertices have degree 3 and in the 3D case all the vertices have degree 4. The γ structure may be constructed by fusing two equilateral triangles, gluing two edges into a single one; the δ structure may follow similar procedure, since it can be constructed by fusing two tetrahedrons, gluing two equilateral triangles into a single one. We consider periodic dispositions of γ and δ on the line, and calculate the ASE in the several cases. The results are displayed in Fig. 14 and

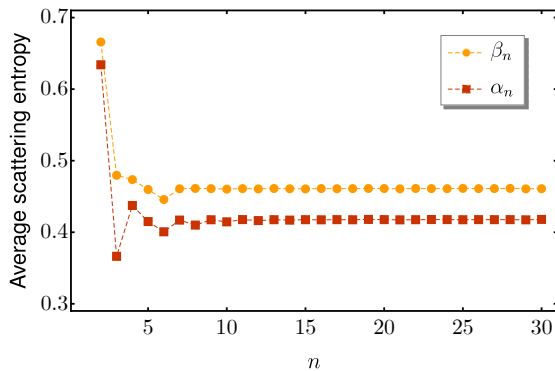


Figure 8: (Color online) Average scattering entropy of the quantum graphs α_n (red) and β_n (yellow) for configurations of the Circle2 type, for several values on n .

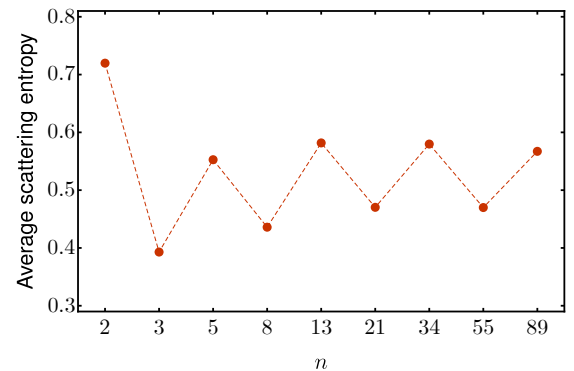


Figure 10: (Color online) Average scattering entropy of quantum graphs on the Circle2 identified by a Fibonacci number.

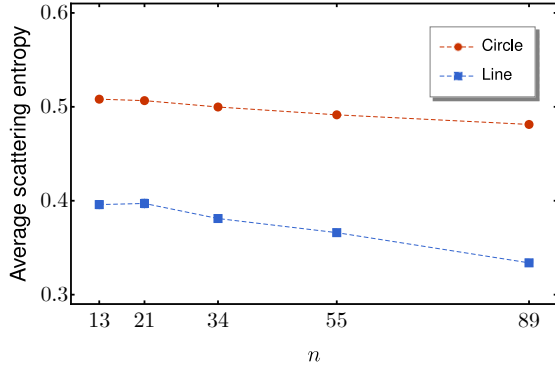


Figure 11: (Color online) Average scattering entropy of quantum graphs in which the degree of the vertices can be 3 or 4, chosen randomly in both the open (blue) and closed (red) arrangements of vertices.

show similar qualitative behavior, with the 3D results being always lower than the 2D ones.

We can suggest several other possible arrangements of the γ and δ structures, in particular, the aperiodic and random dispositions, and this may be implemented following some of the above investigations. However, let us now consider two other families of graphs, one composed of squares in the plane, and the other of regular triangular prisms in space. Since we want to have all the vertices with the same degree to make a fair comparison, in the case of squares, we attach two regular triangular structures to the regular arrangements of squares, and one simple external lead to each one of the two triangles, as illustrated in Fig. 15 with three squares. In the 3D case, we follow similar steps, but now we consider arrangements of regular triangular prisms, attaching two tetrahedrons to their left and right sides and two external leads, as also illustrated in Fig. 15 in the case of three prisms.

We see that in the 2D arrangements, all the vertices have degree 3, and in the 3D cases, all the vertices have degree 4. Recall that we are using regular dispositions of vertices

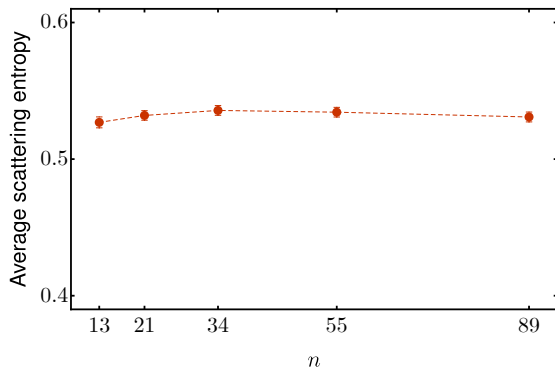


Figure 12: (Color online) Average scattering entropy of quantum graphs with α and β vertices chosen randomly in the Circle2 type of arrangements.

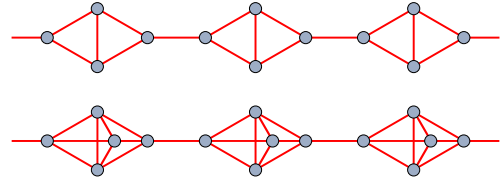


Figure 13: (Color online) Two quantum graphs with three planar γ structures (top) and three spatial δ structures (bottom), which illustrate the general case of periodic structures of the γ_n and δ_n type, respectively.

and edges. We then calculate the ASE for the corresponding QGs and depict the results in Fig. 16 for several squares and prisms, respectively. These two families of QGs give interesting results, with the corresponding ASE being lower for the 3D case. Also, they follow similar behavior, as in Fig. 4, and rapidly diminish, saturating to a constant value as one increases the number of squares and prisms. The 3D study can be seen as a possibility to use the ASE to investigate tube-like configurations of current interest in elastic systems and fluids. Despite the intrinsic difficulty to study 3D systems, recent advancements, in particular, in the study of the transition from a turbulent flow to the case of a coherent flow in three-dimensional active fluids [33] is an interesting motivation.

4. Conclusion

In this work we have investigated the average scattering entropy of quantum graphs in several distinct situations of current interest. The concept was introduced very recently in [3], and it is based on the Shannon entropy [2]. Interestingly, it associates to a given quantum graph a numerical value, in this sense relating the complicated energy-dependent expression for the quantum scattering probability of the quantum graph to a single global quantity. We have studied cases on the line and on the circle with several distinct possibilities, with periodic, aperiodic and random distributions of the vertices. In particular, we noticed that

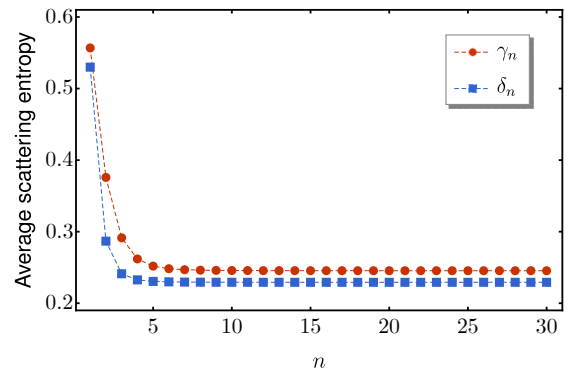


Figure 14: (Color online) Average scattering entropy of quantum graphs for the regular arrangements of the γ structure in 2D and of the δ structure in 3D.

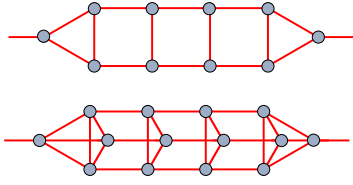


Figure 15: (Color online) Two quantum graphs with three squares (top) and three regular triangular prisms (bottom), which illustrate the general case of periodic structures with squares and prisms, respectively.

the ASE results on the circle are in general higher, when compared to the corresponding results on the line. Also, the numerical values seem not to depend on the number of replications, if there are many replications, but they vary importantly in the case of small structures, with a small number of replications.

We have studied other families of quantum graphs, some of the planar type, and others, having spatial configurations. In the first case, we considered the two possibilities illustrated in Fig. 13. The results are displayed in Fig. 14, and they have a behavior that is qualitatively similar to the case depicted in Fig. 4. They also show that the planar arrangements of vertices always give higher values for the ASE. In the second case, we investigated a planar family of graphs which is described by a regular replication of squares, and the spatial family contains a regular distribution of triangular prisms, see Fig. 15, and they end up with triangles and tetrahedrons, to ensure that all vertices have the very same degree: 3 for the planar case and 4 for the spatial case. The results displayed in Fig. 16 follow similar behavior, with the profiles as the ones depicted in Fig. 4, rapidly diminishing, saturating to a constant value as one increases the number of squares and prisms, respectively.

The diversity of results obtained in this work indicates the feasibility and robustness of the calculations, and they encourage us to further study the subject, hoping that the ASE may become another tool of current interest. We notice, in particular, from the results depicted in Figs. 4, 6,

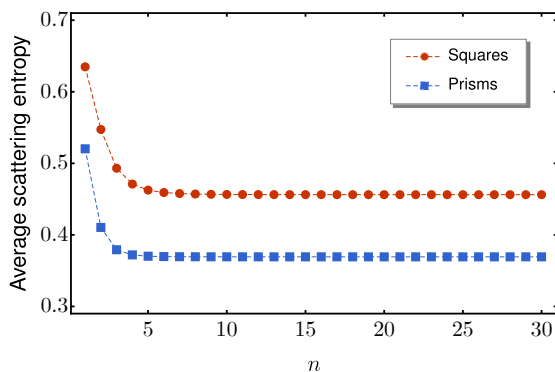


Figure 16: (Color online) Average scattering entropy of quantum graphs for the regular arrangements of squares in 2D and of triangular prisms in 3D.

7, 8, 14 and 16 that the ASE for small structures offers the most large variations, so we think it appears appropriate to use it to study small molecules, for instance, the charge transport through single-molecule junctions, which is quantum mechanical in essence and may provide new tools for the observation of effects that are not accessible in bulk materials; see, e.g., the recent review [29] on single-molecule electronic devices. In this context, if we think of carbon-based molecules, which are made of carbon open chains or lines and/or closed rings or circles, since carbon atoms may form single, double or triple bonds, the study of quantum transport in small molecules suggests that we consider quantum multigraphs, in particular the case of two vertices directly connected by two or three edges.

Other lines of investigation concern the study of the ASE in connection with thermodynamics, statistical and information quantities, such as Rényi and Tsallis entropies, Fisher information and information and geometry [34], to quote some interesting possibilities. Moreover, in [35], for instance, the authors describe the possibility to transfer energy from a cold system to a hot system, with the increase in the Shannon entropy of the memory compensating the decrease in the thermodynamic entropy arising from the flow of heat against a thermal gradient. In the same direction, in [36] another theoretical framework for the thermodynamics of information based on stochastic thermodynamics and fluctuation theorems is presented, where information can be manipulated at molecular or nanometric scales. In another direction, in high energy physics in the study of holography and entanglement entropy, there are many recent works that explore holographic Rényi entropy in conformal field theory [37], gravity dual of Rényi entropy [38], sensitivity to initial conditions in the entanglement of local operators, topological lower bound on quantum chaos [39] and domain wall topological entanglement entropy [40]. Some of the above issues are currently under consideration, and we hope to report on them in the near future.

Acknowledgments

This work was partially supported by the Brazilian agencies Conselho Nacional de Desenvolvimento Científico e Tecnológico (CNPq), Instituto Nacional de Ciência e Tecnologia de Informação Quântica (INCT-IQ), and Paraíba State Research Foundation (FAPESQ-PB, Grant 0015/2019). It was also financed by the Coordenação de Aperfeiçoamento de Pessoal de Nível Superior (CAPES, Finance Code 001). FMA and DB also acknowledge CNPq Grants 434134/2018-0 (FMA), 314594/2020-5 (FMA), 303469/2019-6 (DB) and 404913/2018-0 (DB).

References

- [1] G. Berkolaiko, P. Kuchment, Introduction to Quantum Graphs, American Mathematical Society, 2012.
- [2] C. E. Shannon, W. Weaver, Mathematical Theory of Communication, Combined Academic Publ., 1963. URL: https://www.ebook.de/de/product/3715945/claude_e_shannon_warren_weaver_mathematical_theory_of_communication.html.

- [3] A. A. Silva, F. M. Andrade, D. Bazeia, Average scattering entropy of quantum graphs, *Phys. Rev. A* 103 (2021) 062208.
- [4] F. M. Andrade, S. Severini, Unitary equivalence between the green's function and schrödinger approaches for quantum graphs, *Phys. Rev. A* 98 (2018) 062107.
- [5] F. M. Andrade, A. G. M. Schmidt, E. Vicentini, B. K. Cheng, M. G. E. da Luz, Green's function approach for quantum graphs: an overview, *Phys. Rep.* 647 (2016) 1–46.
- [6] S. Severini, G. Tanner, Regular quantum graphs, *J. Phys. A* 37 (2004) 6675.
- [7] G. K. Tanner, From quantum graphs to quantum random walks, in: *Non-Linear Dynamics and Fundamental Interactions*, volume 213, Springer-Verlag, 2006, pp. 69–87. doi:10.1007/1-4020-3949-2_6.
- [8] Y. Aharonov, L. Davidovich, N. Zagury, Quantum random walks, *Phys. Rev. A* 48 (1993) 1687.
- [9] A. Nayak, A. Vishwanath, Quantum walk on the line, arXiv (2000).
- [10] J. Kempe, Quantum random walks: an introductory overview, *Contemp. Phys.* 44 (2003) 307.
- [11] W. Dür, R. Raussendorf, V. M. Kendon, H.-J. Briegel, Quantum walks in optical lattices, *Phys. Rev. A* 66 (2002) 052319.
- [12] M. C. Marchetti, J. F. Joanny, S. Ramaswamy, T. B. Liverpool, J. Prost, M. Rao, R. A. Simha, Hydrodynamics of soft active matter, *Rev. Mod. Phys.* 85 (2013) 1143–1189.
- [13] D. Needleman, Z. Dogic, Active matter at the interface between materials science and cell biology, *Nat. Rev. Mater.* 2 (2017) 17048.
- [14] Z.-Y. Li, D.-Q. Zhang, S.-Z. Lin, B. Li, Pattern formation and defect ordering in active chiral nematics, *Phys. Rev. Lett.* 125 (2020) 098002.
- [15] A. Alberti, W. Alt, R. Werner, D. Meschede, Decoherence models for discrete-time quantum walks and their application to neutral atom experiments, *New J. Phys.* 16 (2014) 123052.
- [16] M. Gleiser, N. Stamatopoulos, Entropic measure for localized energy configurations: Kinks, bounces, and bubbles, *Phys. Lett. B* 713 (2012) 304–307.
- [17] A. E. Bernardini, R. da Rocha, Informational entropic regge trajectories of meson families in AdS/QCD, *Phys. Rev. D* 98 (2018) 126011.
- [18] N. R. Braga, L. F. Ferreira, R. da Rocha, Thermal dissociation of heavy mesons and configurational entropy, *Phys. Lett. B* 787 (2018) 16.
- [19] N. R. Braga, R. da Mata, Configuration entropy description of charmonium dissociation under the influence of magnetic fields, *Phys. Lett. B* 811 (2020) 135918.
- [20] D. Bazeia, D. Moreira, E. Rodrigues, Configurational entropy for skyrmion-like magnetic structures, *J. Magn. Magn. Mater.* 475 (2019) 734–740.
- [21] D. Bazeia, E. Rodrigues, Configurational entropy of skyrmions and half-skyrmions in planar magnetic elements, *Phys. Lett. A* 392 (2021) 127170.
- [22] N. R. Braga, O. C. Junqueira, Configuration entropy in the soft wall AdS/QCD model and the wien law, *Phys. Lett. B* 820 (2021) 136485.
- [23] R. da Rocha, Information entropy in AdS/QCD: Mass spectroscopy of isovector mesons, *Phys. Rev. D* 103 (2021) 106027.
- [24] R. da Rocha, AdS graviton stars and differential configurational entropy, *Phys. Lett. B* 823 (2021) 136729.
- [25] A. Drinko, F. M. Andrade, D. Bazeia, Narrow peaks of full transmission in simple quantum graphs, *Phys. Rev. A* 100 (2019) 062117.
- [26] A. Drinko, F. M. Andrade, D. Bazeia, Simple quantum graphs proposal for quantum devices, *Eur. Phys. J. Plus* 135 (2020) 451.
- [27] S. Gnutzmann, U. Smilansky, Quantum graphs: Applications to quantum chaos and universal spectral statistics, *Adv. Phys.* 55 (2006) 527.
- [28] G. Tanner, Unitary-stochastic matrix ensembles and spectral statistics, *J. Phys. A: Math. Gen.* 34 (2001) 8485.
- [29] N. Xin, J. Guan, C. Zhou, X. Chen, C. Gu, Y. Li, M. A. Ratner, A. Nitzan, J. F. Stoddart, X. Guo, Concepts in the design and engineering of single-molecule electronic devices, *Nat. Rev. Phys.* 1 (2019) 211–230.
- [30] P. Gehring, J. M. Thijssen, H. S. J. van der Zant, Single-molecule quantum-transport phenomena in break junctions, *Nat. Rev. Phys.* 1 (2019) 381.
- [31] O. Hul, S. Bauch, P. Pakoński, N. Savitsky, K. Życzkowski, L. Sirko, Experimental simulation of quantum graphs by microwave networks, *Phys. Rev. E* 69 (2004) 056205–.
- [32] P. Ribeiro, P. Milman, R. Mosseri, Aperiodic quantum random walks, *Phys. Rev. Lett.* 93 (2004) 190503.
- [33] K.-T. Wu, J. B. Hishamunda, D. T. N. Chen, S. J. DeCamp, Y.-W. Chang, A. Fernández-Nieves, S. Fraden, Z. Dogic, Transition from turbulent to coherent flows in confined three-dimensional active fluids, *Science* 355 (2017) eaal1979.
- [34] S. Ichi Amari, *Information Geometry and Its Applications*, Springer Japan, 2016. doi:10.1007/978-4-431-55978-8.
- [35] D. Mandal, H. T. Quan, C. Jarzynski, Maxwell's refrigerator: An exactly solvable model, *Phys. Rev. Lett.* 111 (2013) 030602.
- [36] J. M. R. Parrondo, J. M. Horowitz, T. Sagawa, Thermodynamics of information, *Nat. Phys.* 11 (2015) 131–139.
- [37] X. Dong, The gravity dual of rényi entropy, *Nat. Commun.* 7 (2016) 12472.
- [38] X. Dong, Shape dependence of holographic rényi entropy in conformal field theories, *Phys. Rev. Lett.* 116 (2016) 251602.
- [39] Z. Gong, L. Piroli, J. I. Cirac, Topological lower bound on quantum chaos by entanglement growth, *Phys. Rev. Lett.* 126 (2021) 160601.
- [40] B. Shi, I. H. Kim, Domain wall topological entanglement entropy, *Phys. Rev. Lett.* 126 (2021) 141602.